THE JOURNAL OF BIOLOGICAL CHEMISTRY VOL. 289, NO. 15, pp. 10345–10358, April 11, 2014

Nitrite Reductase and Nitric-oxide Synthase Activity of the Mitochondrial Molybdopterin Enzymes mARC1 and mARC2*

Received for publication, January 31, 2014 Published, JBC Papers in Press, February 5, 2014, DOI 10.1074/jbc.M114.555177

Courtney E. Sparacino-Watkins[‡§1], Jesús Tejero[‡], Bin Sun[‡§], Marc C. Gauthier[‡§], John Thomas[¶], Venkata Ragireddy[‡], Bonnie A. Merchant[‡], Jun Wang[‡], Ivan Azarov[‡], Partha Basu[¶], and Mark T. Gladwin[‡§2]

From the [‡]Vascular Medicine Institute, University of Pittsburgh, Pittsburgh, Pennsylvania 15261, [§]Division of Pulmonary, Allergy, and Critical Care Medicine, University of Pittsburgh, Pittsburgh, Pennsylvania 15213, and [¶]Department of Chemistry and Biochemistry, Duquesne University, Pittsburgh, Pennsylvania 15282

Background: Nitrite reduction pathways are critical for biological NO production under hypoxia.
Results: The mitochondrial enzyme mARC reduces nitrite to NO using cytochrome b_5 as electron donor.
Conclusion: mARC forms an electron transfer chain with NADH, cytochrome b_5, and cytochrome b_5 reductase to reduce nitrite to NO.
Significance: mARC proteins may constitute a new pathway for hypoxic NO production *in vivo*.

Mitochondrial amidoxime reducing component (mARC) proteins are molybdopterin-containing enzymes of unclear physiological function. Both human isoforms mARC-1 and mARC-2 are able to catalyze the reduction of nitrite when they are in the reduced form. Moreover, our results indicate that mARC can generate nitric oxide (NO) from nitrite when forming an electron transfer chain with NADH, cytochrome b_5, and NADH-dependent cytochrome b_5 reductase. The rate of NO formation increases almost 3-fold when pH was lowered from 7.5 to 6.5. To determine if nitrite reduction is catalyzed by molybdenum in the active site of mARC-1, we mutated the putative active site cysteine residue (Cys-273), known to coordinate molybdenum binding. NO formation was abolished by the C273A mutation in mARC-1. Supplementation of transformed *Escherichia coli* with tungsten facilitated the replacement of molybdenum in recombinant mARC-1 and abolished NO formation. Therefore, we conclude that human mARC-1 and mARC-2 are capable of catalyzing reduction of nitrite to NO through reaction with its molybdenum cofactor. Finally, expression of mARC-1 in HEK cells using a lentivirus vector was used to confirm cellular nitrite reduction to NO. A comparison of NO formation profiles between mARC and xanthine oxidase reveals similar K_{cat} and V_{max} values but more sustained NO formation from mARC, possibly because it is not vulnerable to autoinhibition via molybdenum desulfuration. The reduction of nitrite by mARC in the mitochondria may represent a new signaling pathway for NADH-dependent hypoxic NO production.

Nitric oxide (NO) is a potent vasodilator and a pleiotropic signaling molecule (1). Two distinct biochemical pathways generate NO in mammals: the nitric oxide synthase-dependent pathway and the inorganic nitrate-nitrite-NO pathway (2). The nitric oxide synthase-dependent pathway has been thoroughly characterized. Nitric oxide synthase oxidizes L-arginine with molecular oxygen, forming NO and citrulline. The later pathway is characterized by a two-step metabolism of nitrate (NO_3^-) to nitrite (NO_2^-), then NO_2^- to NO. The nitric oxide synthase enzymes require molecular oxygen and are oxidative, whereas the inorganic nitrate-nitrite-NO pathway is oxygen-independent and reductive. Nitrate reduction to nitrite primarily requires commensal oral bacteria that express nitrate reductase enzymes (3). Nitrite reduction can be catalyzed by the mammalian mitochondria (4, 5) and several enzymatic nitrite reductase systems (6, 7). Determination of the mammalian nitrite reductase pathways is of great interest for human health and disease, as the effects of nitrite are largely mediated by its reduction to NO (2).

The role of NO and NO_2^- in regulation of mitochondrial function have been extensively studied (8–10). NO regulates mitochondrial function through direct inhibition of cytochrome *c* oxidase, which in turn inhibits mitochondrial oxygen consumption (10). It is not clear if nitrite is directly reduced to NO by the mitochondria or if NO_2^- metabolites interact with the mitochondria (8). Mitochondrial cytochrome *c* (11), complex III (5), and complex IV (10) have been reported to reduce nitrite into NO as well as mitochondria-associated deoxymyoglobin and ubiquinol (9). In this study we investigate a novel mitochondrial enzyme, mitochondrial amidoxime-reducing component (mARC),[3] as a NO-forming nitrite reductase.

mARC was renamed mitochondrial amidoxime reducing component in 2006 after researchers identified this novel molybdopterin enzyme as the catalytic subunit in a three-pro-

* This work was supported, in whole or in part, by National Institutes of Health Grants HL098032, HL096973, and DK085852. This work was also supported by the Institute for Transfusion Medicine and the Hemophilia Center of Western Pennsylvania (to M. T. G.) and by the Competitive Medical Research Fund of the UPMC Health System (to J. T.).
[1] Supported by National Institute of Health Institutional Training Grant 2T32HL007563-26 (to the division of Pulmonary, Allergy, and Critical Care Medicine at the University of Pittsburgh).
[2] To whom correspondence should be addressed: E1244 Biomedical Science Tower, 200 lothrope St., Division of Pulmonary, Allergy, and Critical Care Medicine, University of Pittsburgh, Vascular Medicine Institute, University of Pittsburgh, Pittsburgh, PA 15261. Tel.: 412-624-8725; Fax: 412-648-3181; E-mail: gladwinmt@upmc.edu.

[3] The abbreviations used are: mARC, mitochondrial amidoxime reducing component; XO, xanthine oxidase; AO, aldehyde oxidase; CYB5, cytochrome b_5; CYB5R, cytochrome b_5 reductase; CYB5B, cytochrome b_5 type b; W-mARC, tungsten mARC; Bis-Tris, 2-[bis(2-hydroxyethyl)amino]-2-(hydroxymethyl)propane-1,3-diol; NOA, nitric oxide analyzer.

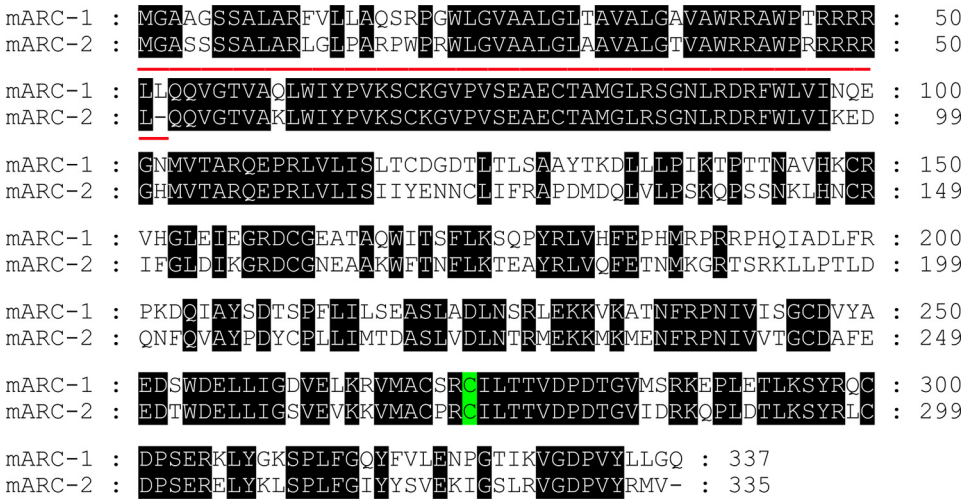

FIGURE 1. **Alignment of full-length human mARC-1 (NP_073583.3; 337 amino acid residues) and mARC-2 (NP_060368.2; 335 amino acid residues).** Identical residues are represented with *black shading* and in *white font*. The mitochondrial targeting sequence (amino acids 1–51) is *underlined* in *red*. Cysteine 273 (*mARC-1*) and cysteine 272 (*mARC-2*), which coordinate molybdenum in the active site, are highlighted in *green*.

tein amidoxime reducing chain (12). The other two proteins, cytochrome b_5 (CYB5) and cytochrome b_5 reductase (CYB5R), catalyze electron transfer from NADH to the terminal oxidoreductase, mARC (12). Humans encode two mARC genes, mARC-1 and mARC-2, located in tandem on chromosome 1. Approximately 65% sequence identity is conserved between the two enzymes (Fig. 1) (13). The N termini (1–52 amino acids in mARC-1) of mARC-1 and mARC-2 contain a mitochondrial targeting signal followed by a transmembrane helix. The C-terminal section (53–337 amino acids in mARC-1) contains catalytic core and a molybdopterin binding site (14).

Despite the ability of mARC to catalyze reduction of amidoxime groups *in vitro*, the physiological function of mARC is not clear. Our new results indicate that mARC can also catalyze the reduction of nitrite to NO with NADH in the presence CYB5 and CYB5R and that the molybdopterin active site is the location for nitrite reduction to NO. These data provide biochemical evidence for an alternative function of mARC in nitrite-NO signaling.

EXPERIMENTAL PROCEDURES

Reagents and Standard Sample Preparation—All chemicals were purchased from Sigma unless otherwise noted. Spectrophotometric measurements were performed with an Agilent 8453 or a Cary 50 spectrophotometer. The sequence of all DNA constructs was determined at the University of Pittsburgh Genomics and Proteomics Core Laboratory by standard techniques. Concentrations of CYB5 and CYB5R were measured by UV-visible spectroscopy using the published extinction coefficients for CYB5 ($\epsilon^{414\,nm} = 117\ mM^{-1}{\cdot}cm^{-1}$) (15) and CYB5R ($\epsilon^{462\,nm} = 10.4\ mM^{-1}{\cdot}cm^{-1}$) (16), respectively. Molybdenum content was determined by inductively coupled plasma optical emission spectroscopy at the Center for Applied Isotope Studies (University of Georgia). Chromatographic separations were conducted with an Äkta-Purifier FPLC (GE Healthcare) running Unicorn software Version 5.1. For each chromatographic separation the resin of choice was packed into a XK 26/20 column (GE Healthcare). Protein identity was confirmed with liquid chromatography and tandem mass spectrometry (University of Pittsburgh Genome and Protein Core Facilities).

Cloning, Expression, and Purification of Human Cytochrome b_5 Reductase—Standard molecular biology techniques were used to clone the human CYB5R gene into the pET28a plasmid (Novagen). PCR was used to amplify the coding sequence of the 278 amino acid CYB5R3 isoform 2 (accession number NP_015565.1) from cDNA (LIFESEQ3585709, Open Biosystems) and to incorporate flanking restriction enzyme cleavage sites (NdeI and HindIII). The oligonucleotide sequences for the forward and reverse primers are 5′-ATA AAC ATA TGA AGC TGT TCC AGC GCT CC-3′ and 5′-ATA AAA AGC TTA GAA GAC GAA GCA GCG CTC-3′, respectively. CYB5R thus cloned includes an N-terminal hexahistidine (His_6) tag. The plasmid was transformed into SoluBL21 cells (Genlantis). Expression and purification were performed as previously published, with minor modifications (16). Cells were grown on terrific broth media with 30 $\mu g{\cdot}ml^{-1}$ kanamycin at 30 °C for 20 h post-induction with 1 mM isopropyl-β-D-thiogalactopyranoside. Affinity purification was performed using nickel-nitrilotriacetic acid superflow resin (Qiagen) as instructed by the manufacturer. The eluted protein was concentrated and dialyzed with ultrafiltration (10-kDa molecular mass cutoff, Millipore) against 50 mM Tris-HCl, pH 7.4, to remove imidazole. The aliquoted protein was stored at −80 °C in buffer containing 50 mM Tris-HCl, pH 7.4, 150 mM NaCl, and 10% glycerol.

Expression and Purification of Human Cytochrome b_5—Recombinant human cytochrome b_5 type b (CYB5B) (accession number NP_085056.2) was isolated from *Escherichia coli* strain SoluBL21 (Genlantis). The expression plasmid (pET11a:CYB5) was kindly provided by Mario Rivera (University of Kansas) (17). The transformed SoluBL21 cells were grown on terrific broth media supplemented with 100 μg/ml ampicillin and δ-aminolevulinic acid (0.4 mM) until the optical density at 600 nm reached 0.8 absorbance units. Expression was induced with 1 mM isopropyl-β-D-thiogalactopyranoside and then incubated at 37 °C for 4 h. Isolation of human CYB5B was conducted as

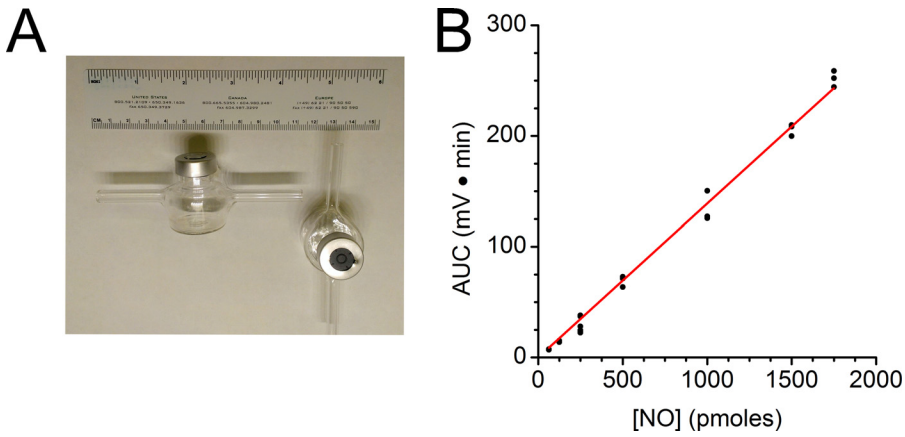

FIGURE 2. *A*, photograph of the custom glass purge vessel used for NO analyses with the nitric oxide analyzer. *B*, standard curve used to calculate nitric oxide concentration with nitrite standard injections into the triiodide (I_3^-) gas phase chemiluminescence assay. $y = 0.139$.

previously reported, (17) with minor modifications to the chromatographic separation; specifically, we used the DE32 anion exchange resin (Whatman) with the previously described Äkta-Purifier FPLC system. CYB5 eluted with a gradient from 10 to 300 mM NaCl in 50 mM Tris-HCl, pH 8.0. CYB5B eluted at ~150 mM NaCl. High molecular mass proteins were removed by passing the eluted fractions through a 30-kDa molecular mass cutoff filtration membrane (Millipore) before concentration with a 10-kDa molecular mass cutoff filter (Millipore). The aliquoted protein was stored at −80 °C in 50 mM Tris-HCl buffer at pH 7.4.

Cloning, Expression, and Purification of Human mARC-1 and mARC-2—The recombinant mARC-1 and mARC-2 expression plasmid (pET28a-mARC) was constructed as described for CYB5R. The mARC-1 and mARC-2 genes were amplified with PCR from cDNA (clone IDs 3872779 and 3458649, Open Biosystems), then inserted into the pET28a vector using the NdeI and HindIII restriction sites, in-frame with the N-terminal His_6 coding sequence. The following oligonucleotides were used to amplify the protein coding mARC sequences and to insert flanking NdeI and HindIII restriction enzyme sites: 5′-ATA TAT CAT ATG GGC GCC GCC GGC TCC TCC GCG-3′ (forward mARC-1), 5′-AAA TTT AAG CTT TTA CTG GCC CAG CAG GTA CAC AGG-3′ (reverse mARC-1), 5′-ATA TAT CAT ATG GGC GCT TCC AGC TCC TCC GCG-3′ (forward mARC-2), and 5′-CAT AAT TAA GCT TCT ACA CCA TCC GAT ACA CAG GGT C-3′ (reverse mARC-2).

The N-terminal mitochondrial targeting sequence (Fig. 1) was removed during the cloning, as previously published (13), yielding a coding sequence corresponding to mARC-1 amino acid residues 53–337 (NP_073583.3) and mARC-2 residues 52–335 (NP_060368.2). *E. coli* strain SHuffle® pLysS (New England Biolabs) was transformed with pET28a-mARC and a second plasmid, pTPR1. pTPR1 contains the *E. coli* genes for eukaryotic molybdopterin biosynthesis (provided by Tracy Palmer, University of Dundee). Cells were grown on terrific broth media supplemented with 30 $\mu g \cdot ml^{-1}$ kanamycin, 15 $\mu g \cdot ml^{-1}$ tetracycline, 33 $\mu g \cdot ml^{-1}$ chloramphenicol, and 1 mM sodium molybdate at 37 °C until the absorbance at 600 nm was ~0.8. Protein expression was then induced by the addition of isopropyl-β-D-thiogalactopyranoside (1 mM). Cells were incubated at 30 °C for 20 h post-induction and then collected by centrifugation. To generate the tungsten mARC (W-mARC), growth medium was supplemented with 3 mM tungstate instead of molybdate as reported previously (18). Chromatographic isolation was conducted with nickel-nitrilotriacetic acid superflow (Qiagen) as instructed by the manufacturer. Bis-Tris acetate (50 mM) was used as buffer in all steps. The eluted protein was concentrated by ultrafiltration (10-kDa molecular mass cutoff) and dialyzed against 50 mM Bis-Tris buffer, pH 7.4, containing 150 mM NaCl to remove imidazole.

Mutagenesis of Recombinant mARC-1—Site-directed mutagenesis was performed using the QuikChange II kit (Stratagene). The wild type recombinant mARC expression plasmid (pET28-mARC) previously described was used as the template for the generation of the active site mARC-1 mutant. The oligonucleotides used to mutate the mARC-1 active site cysteine residue to alanine were 5′-GTG ATG GCT TGT TCC AGA GCG ATT TTA ACC ACA GTG GAC-3′ and 5′-GTC CAC TGT T GG TTA AAA TCG CTC TGG AAC AAG CCA TCA C-3′. Mutations were confirmed by DNA sequencing. Expression and purification were then conducted using the same procedure as the wild type recombinant mARC.

Determination of Nitric Oxide Formation Rates—A Sievers Nitric Oxide Analyzer 208i (GE Healthcare) was used to monitor NO production by chemiluminescence. Liquid software (Version 3) was used to monitor and collect data. The factory supplied purge vessel (GE Healthcare) was used for the experiments with dithionite and mARC. Data were collected and analyzed as published (19–21). A second, custom-made vessel was used for experiments with NADH, mARC, CYB5, and CYB5R because the purge vessel could not be used for sequential addition of enzymes. The custom-made glass vessel, referred as the non-purge vessel from this point on, was modeled after a published design (22) and created at the University of Pittsburgh glass-blowing facility (Fig. 2*A*). The key difference among the purge and non-purge vessels is the path of carrier gas. Gas flows horizontally over the head space of the enzyme reaction in a sealed vessel in the non-purge system. In the purge system, gas flow is horizontal and bubbles through the enzyme reaction mixture. Each reaction vessel was calibrated with known amounts of sodium nitrite using the triiodide (I_3^-) assays, as

published (23). The calibration data collected with the non-purge vessel are provided in Fig. 2*B*. Argon was used as carrier gas for all nitric oxide analyzer (NOA) assays unless otherwise noted.

Enzymes assays were performed in 50 mM Bis-Tris acetate buffer at pH 7.4 unless otherwise noted. Buffers were purged with argon to remove oxygen before the addition of enzyme. Reagent and enzymes were injected into the reaction vessel through butyl rubber septa using a gas-tight Hamilton syringe. Unless noted otherwise, mARC (1–3 μM) was injected last. For each reaction, data were collected for at least 10 min. Raw data from the NOA was transferred into Origin Lab software (Version 8.6) to calculate NO formation rates. The data were first integrated first to adjust for total NO accumulation, as gas-phase chemiluminescence measures transient NO as the carrier gas (argon) is passed through the reaction vessel to the NO detector. Next, the integrated NO signal (mV·min) was converted to NO concentration (pmol min) using the equation derived from the previously described NO calibration ($y = 0.1389x$). The slope of the integral, which corresponds to the plateau region of the raw data, was used as the rate of NO formation. All data fitting was performed with Origin Lab software.

mARC-2 Overexpression in Human Embryonic Kidney (HEK) Cells—The complete 335-amino acid mARC-2 gene sequence (NP_060368.2), including the mitochondrial target, was included in the HEK cell expression studies to preserve the natural protein maturation process and subcellular localization. The 1618-bp human mARC-2 gene was amplified with PCR from cDNA (clone ID 3458649, Open Biosystems) then inserted into the pLVX-AcGFP1-N1 (Clontech) vector using the XhoI and EcoRI restriction sites in-frame with the C-terminal *Aequorea coerulescens* GFP coding sequence. The following oligonucleotides were used to amplify the protein coding mARC sequences and to insert flanking XhoI and EcoRI restriction enzyme sites: CCA TCT CGA GCC TCG CTC TGC CAT GG (forward) and CAG AAT TCT CAC CAT CCG ATA CAC AGG (reverse). Cloning was conducted as previously described, and the sequence of each construct was confirmed with DNA sequencing.

The lentiviruses were packaged according to the manufacturer's instructions (Invitrogen, ViraPower Lentiviral packing mix). The HEK 293 cells were then infected with lentivirus and selected with puromycin (20 ng/ml) for at least 2 weeks. For experiments, cells were grown to confluence in 17-cm plastic Petri dishes, then collected by centrifugation and washed before flash freezing with liquid nitrogen. Cells were suspended in 50 mM Bis-Tris buffer, pH 7.4, with 200 mM NaCl then lysed with sonication. Each NO formation assay data contained 60–100 mg of total protein.

mARC-2 expression was measured by SDS/PAGE and Western blot using standard techniques. The nitrocellulose membrane was incubated with anti-mARC-2 (Sigma) or anti-GFP (Clontech) overnight at 4 °C. Goat anti-mouse IRDye 680 (LI-COR Biosciences) was used for detection, and images were recorded with an imaging system (Odyssey).

RESULTS

Recombinant Human mARC-1 and mARC-2 Enzyme Isolation—To obtain sufficient quantities of mARC enzyme for kinetic analysis, we produced recombinant human mARC-1 and mARC-2 in *E. coli*. We removed the mitochondrial translocation motif of mARC-1 and mARC-2 and replaced it with a His_6 N-terminal tag creating recombinant proteins of ~35 kDa. On average, 10 mg of recombinant mARC were isolated per liter of *E. coli* culture. Assuming a theoretical value of 1 mol of molybdenum/mol of mARC enzyme, mARC-1 had an ~60% molybdenum incorporation and mARC-2 an 80% molybdenum incorporation, as measured by inductively coupled plasma optical emission spectroscopy. The identities of the isolated mARC-1 and mARC-2 enzymes were verified by mass spectrometry.

Nitrite Is Reduced to NO by Dithionite-reduced mARC-1 and mARC-2—To confirm the ability of human mARC-1 and mARC-2 to catalyze nitrite reduction, NO formation rates were measured with chemiluminescence-based NO detection. This is the standard method used to characterize nitrite-reducing molybdenum enzymes, such as xanthine oxidase, and aldehyde oxidase (20, 21, 24) and thus is a reasonable basis for comparing mARC rates with published literature.

We started with a simple one-enzyme assay that contained dithionite-reduced mARC and nitrite (Fig. 3*A*). Both mARC-1 and mARC-2 can generate NO from nitrite in the presence of dithionite. To verify that the formation of NO was due to the mARC protein and not to direct nitrite reduction by dithionite, mARC enzymes were added 90 s after the addition of dithionite (Fig. 3, *B* and *C*). The background rate of NO formation before the injection of mARC was recorded. Interestingly, the two enzymes appeared to have different NO formation profiles; mARC-1 displayed a broad low intensity signal (Fig. 3*B*), whereas mARC-2 generated a sharp high intensity peak of NO (Fig. 3*C*). NO formation is dependent on the presence of active enzyme, as heat-denatured mARC-1 or mARC-2 abolished NO formation in the presence of 1000 μM nitrite (orange traces in Fig. 3, *D* and *E*, respectively). The observed rates of NO formation were fitted to the Michaelis-Menten equation (Fig. 3*F*). From these data the apparent Michaelis-Menten constant (K_m) for nitrite and the maximum rate (V_{max}) of NO-production were estimated to be 0.6 mM and 2.3 nmol of $NO{\cdot}s^{-1}{\cdot}mg^{-1}$, respectively, for mARC-1 and 0.2 mM and 3.3 nmol $NO{\cdot}s^{-1}{\cdot}mg^{-1}$, respectively, for mARC-2. mARC-1 and mARC-2 share significant sequence similarities; therefore, we focused our full evaluation on mARC-1, with reproduction of critical experiments with mARC-2.

mARC-1 Forms a Nitrite Reductase Metabolon with CYB5, CYB5R, and NADH—Kotthaus *et al.* (25) previously demonstrated that mARC-1 and mARC-2 can accept electrons from NADH via CYB5 and CYB5R. We evaluated NO formation rates with recombinant mARC-1 in the presence of CYB5, CYB5R, and NADH. A diagram summarizing this relationship is presented in Fig. 4*A*. NO production was only observed in the presence of the complete reductase system (Fig. 4*B*); omission of any component abolished NO generation. We studied the

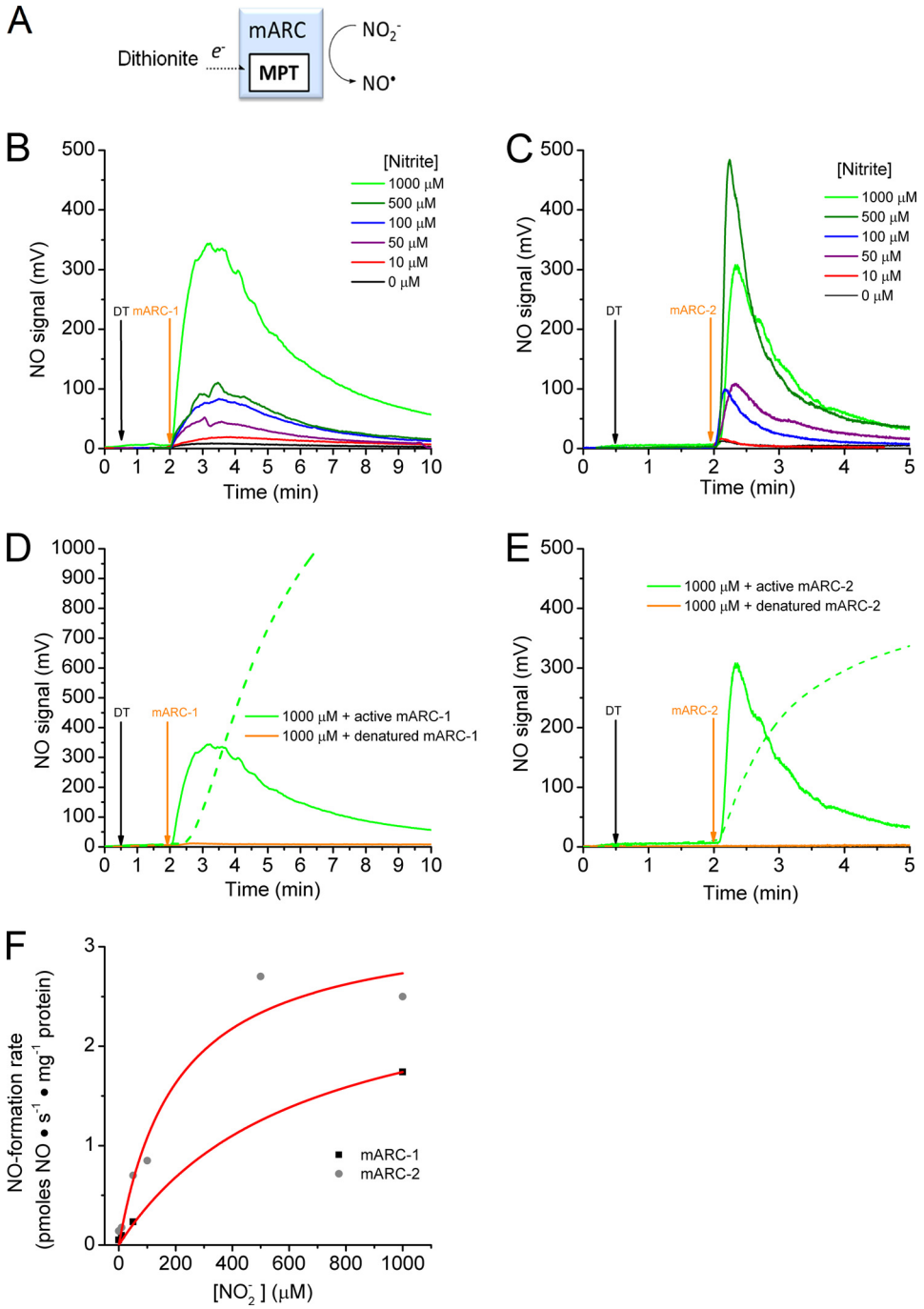

FIGURE 3. **NO formation from nitrite by dithionite-reduced mARC-1 and mARC-2.** *A*, schematic diagram of electron transport from dithionite directly to mARC. *Panels B–D* display representative raw data of NO formation (mV) over time (minutes) collected with the NOA using dithionite-reduced recombinant mARC-1 (*B* and *D*) or mARC-2 (*C* and *E*). *MPT*, molybdopterin. First, data were collected with buffer and nitrite ($t = 0$ min); next, dithionite was injected (*black arrows* at $t = 0.5$ min.); last, mARC enzyme was injected (*orange arrows*, $t = 2$ min). Increasing nitrite concentration escalated NO signal (*B* and *C*). Heat-denatured mARC-1 (*D*) or mARC-2 (*E*) did not produce NO from nitrite. Total NO formed over time (integral) is represented with a *green dashed line* in *D* and *E*. *F*, observed NO production rates (pmol of $NO{\cdot}s^{-1}{\cdot}mg^{-1}$ mARC) were plotted *versus* nitrite concentration (μM) and then fit with the Michaelis-Menten function. The apparent K_m and V_{max} were estimated for mARC-1 (636 ± 139 μM nitrite and 2.3 ± 0.3 nmol of $NO{\cdot}s^{-1}{\cdot}mg^{-1}$, respectively) and mARC-2 (204 ± 84.4 μM nitrite and 3.3 ± 0.4 nmol $NO{\cdot}s^{-1}{\cdot}mg^{-1}$, respectively). Each assay contained 50 mM Bis-Tris buffer, pH 7.4, sodium dithionite (600 μM), mARC-1 (3 μM), or mARC-2 (1 μM) at 25 °C.

rates of NO formation in a nitrite range (1–60 mM) similar to that observed for other molybdenum enzymes (xanthine oxidase, and aldehyde oxidase) (20, 21, 24). NO formation escalates with increasing nitrite concentrations (Fig. 4 *C* and *D*), and NO formation kinetics exhibited a pattern consistent with the Michaelis-Menten equation (Fig. 4*E*). From these data, the K_m for nitrite was determined to be 9.5 ± 1.5 mM, and the V_{max} of NO-production was calculated to be 3.60 ± 1.5 nmol $NO{\cdot}s^{-1}{\cdot}mg^{-1}$ mARC-1. These values are similar to published NO formation kinetics derived from xanthine oxidase and aldehyde oxidase (Table 1), which have been shown to physiologically regulate nitrite reduction to NO (20, 21, 24).

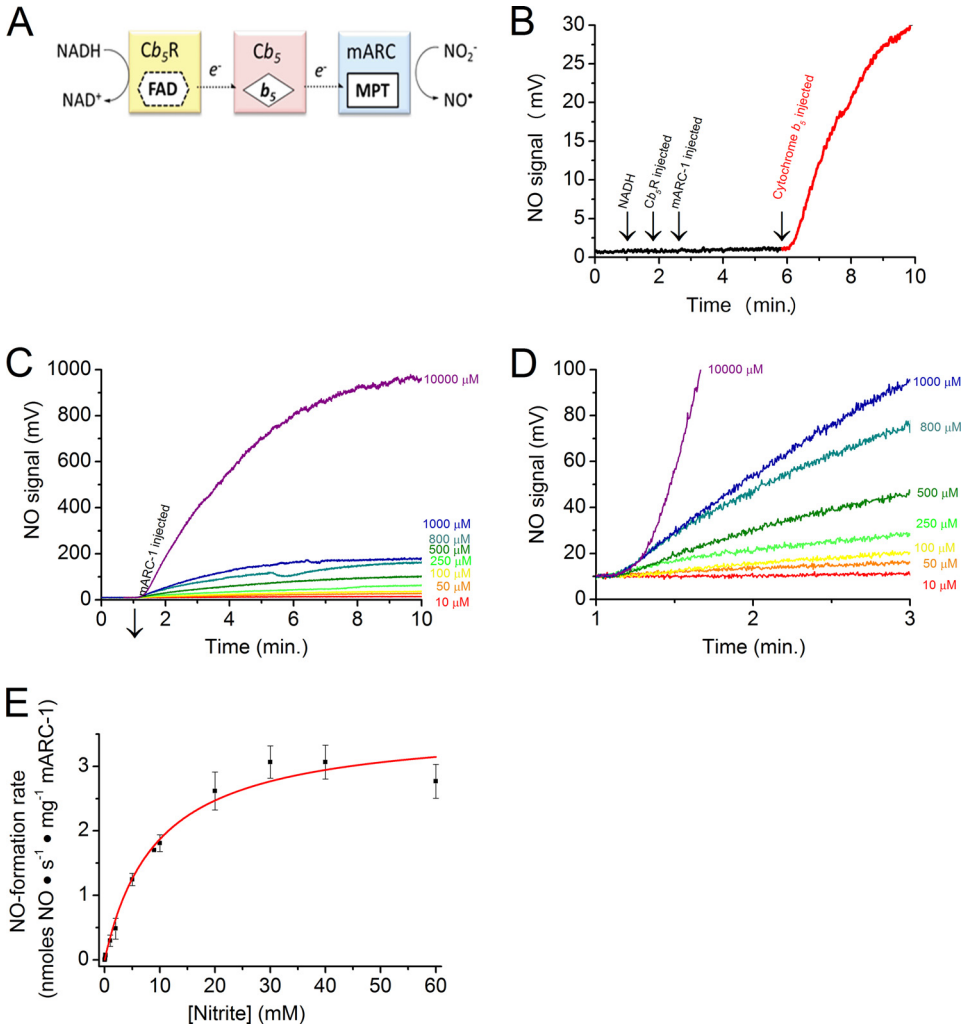

FIGURE 4. **Effect of nitrite concentration on NO production from the mARC-1 reductase system.** *A*, schematic diagram of electron transport from NADH to mARC through CYB5R and CYB5. *MPT*, molybdopterin. *B*, raw data showing NO signal (mV) over time, starting with nitrite (100 μM) in buffer and sequential injections of NADH, CYB5R (*Cb_5R*), mARC-1, and CYB5 (*black arrows*). *C*, representative raw data collected from the NOA at different nitrite concentrations. *D*, magnification of the low nitrite data presented in *panel C*. *E*, calculated rate of NO-production (nmol NO·s^{-1}·mg^{-1} mARC-1) *versus* nitrite concentration (mM). Assays contained NADH (1 mM), mARC-1 (1–3 μM), CYB5 (2 μM), CYB5R (0.2 μM), and Bis-Tris buffer (50 mM if $NO_2^- < 10$ mM or 200 mM if $NO_2^- \geq 10$ mM) at pH 7.4 and 37 °C. $n = 3$. Data were fit with the Michaelis-Menten equation. The K_m was determined to be 8.2 mM, and the V_{max} was 3.5 nmol of NO·s^{-1}·mg^{-1} mARC-1.

TABLE 1

Molybdopterin nitrite reductase enzymes: XO, AO, and mARC

MO, molybdenum.

Enzyme	Redox active cofactors	Electron donor	Kinetic constants			Reference
			K_m	NO formation rates	K_{cat}	
			mM NO_2^-	*nmol·$s^{-1}$$mg^{-1}$*	*s^{-1}*	
XO	MO 2Fe-2S FAD	NADH	2	0.92	0.3	20
			22.9 ± 8.1	62 ± 12		24
AO	MO 2Fe-2S FAD	NADH	2.7	8.5[a]		21
mARC-1	MO[b]	NADH	9.5 ± 1.5	3.60 ± 1.5	0.1	This work
mARC-1 (C273A)	MO[b]	NADH	NA[c]	<0.01	~0	
W- mARC-1	W[b]	NADH	NA	<0.01	~0	

[a] Units = nmol·s^{-1}·$unit^{-1}$.
[b] Reaction mixture includes b_5-type heme (CYB5) and FAD (CYB5R).
[c] NA, not applicable.

NO Formation from Nitrite Is Limited by mARC-1 Concentration, Not NADH, CYB5, or CYB5R—To exclude the possibility that other components of the reaction (*i.e.* NADH, CYB5, or CYB5R) were rate-limiting, we systematically varied the concentrations of each component and then measured NO formation rates (Fig. 5). Increasing mARC-1 concentration increases NO production linearly (Fig. 5*A*), indicating that mARC concentration is rate-limiting. Conversely, concentrations of CYB5, CYB5R, and NADH were not rate-limiting (Fig. 5, *B*, *C*, and D, respectively). These data show a non-linear response to increasing concentrations of CYB5, CYB5R, or NADH. We calculated the apparent K_m by fitting the data to the Michaelis-Menten equation. The apparent K_m values (CYB5 = 0.08 ± 0.02 μM, CYB5R = 0.007 ± 0.002 μM, and NADH = 6.5 ± 1.6

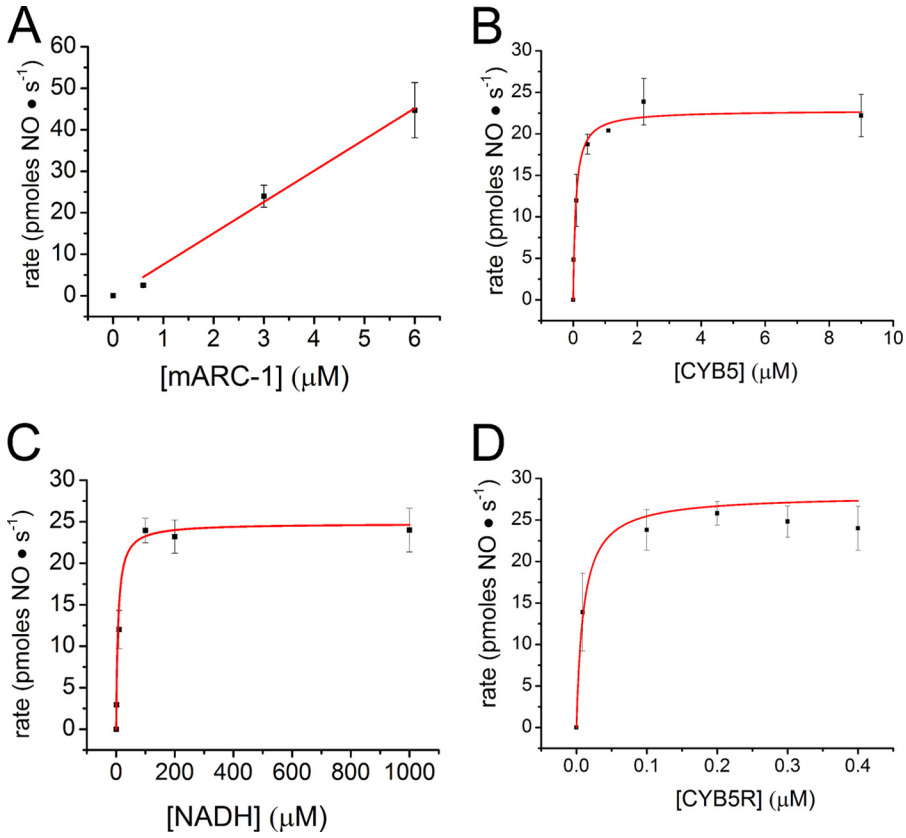

FIGURE 5. **NO production rates (pmol of NO·s^{-1}) *versus* concentration of mARC-1 ($y = 7.5$) (*A*), CYB5 ($K_m = 0.08$ μM, $V_{max} = 22.8$ pmol of NO·s^{-1}) (*B*), NADH ($K_m = 6.5$ μM; $V_{max} = 24.8$ pmol of NO·s^{-1}) (*C*), and CYB5R ($K_m = 0.007$ μM; $V_{max} = 25.6$ pmol NO·s^{-1}) (*D*).** Unless noted otherwise, assays contained Bis-Tris (50 mM), pH 7.4, NADH (1 mM), nitrite (1 mM), mARC-1 (3 μM), CYB5 (2 μM), and CYB5R (0.2 μM) at 37 °C; $n = 3$. Linear regression was used to derive the slope in *panel C*. Data in *D–F* was fit with the Michaelis-Menten equation.

μM) are much lower than our working ranges, indicating that these components are not rate-limiting and are likely to reduce mARC under physiological conditions.

Determination of the Molybdopterin Nitrite Reductase Active Site of mARC-1—After establishing that nitrite reduction to NO requires reduced mARC either through the NADH-dependent mitochondria complex with CYB5 and CYB5R or via non-specific electron donors, such as dithionite, we wanted to determine if nitrite reduction occurred in the molybdopterin active site of human mARC-1. Therefore, we generated a tungsten (W)-substituted mARC-1 (W-mARC-1) and the mutant C273A recombinant mARC-1. The strictly conserved putative active site cysteine was mutated to alanine in an effort to disrupt catalytic turnover at the molybdenum active site (Fig. 6*A*). Both mARC-1 variants were expressed in *E. coli* and purified as described for the wild-type enzyme (Fig. 6*B*). The UV-visible spectrum of wild-type mARC is similar to the previously published spectra (13). Comparison of the W-mARC-1, C273A, and wild type mARC-1 UV-visible spectra indicates spectral differences (Fig. 6*C*). The exact molecular basis of the 340-nm stretch is not clear; however, the molybdopterin is certainly the source (26). Molybdenum content of the two mARC-1 variants was measured by atomic absorption. The C273A mutant maintained molybdenum content (~40%), albeit less than the wild type (~60%). As expected, the W-mARC-1 contained no molybdenum, reflecting replacement by tungsten (W). Nitrite reduction and NO formation was abolished in C273A mARC-1 and W-mARC-1 (Fig. 6, *D* and *E*). Therefore, we conclude that mARC-1 reduces nitrite to NO in the molybdenum active site, and Cys-273 is an integral amino acid of this site, presumably required for direct coordination to the molybdenum. Assuming the mARC active site is the same as sulfite oxidase, as predicted (27), removing the molybdenum coordinating cysteine ligand probably produce an oxygen-coordinated ligand (from water) (28). This mutation of the active site cysteine to alanine in sulfite oxidase family enzymes abolishes catalytic activity and has been demonstrated with sulfite oxidase (28), *Chlamydomonas reinhardtii* ARC (29), and similar molybdopterin enzymes.

Effect of pH on NO Formation Rates by mARC-1—We evaluated the effect of proton concentration on nitrite reductase activity, as nitrite reduction to NO requires protons and electrons. Decreasing the pH by 1 unit causes an ≈10-fold rate increase in nitrite reduction by heme-containing proteins such as hemoglobin, myoglobin, and neuroglobin (30–32). This can be interpreted as a direct reaction of nitrous acid with the heme, as previously proposed (31, 33). Xanthine oxidase and aldehyde oxidase do not show this direct relationship between rate and proton concentration, although lower pH does increase the rate of the reaction (19, 21, 34, 35). mARC-1 exhibited a similarly limited change in the reaction rates, with only a 3-fold change in rate at pH 7.4 *versus* 6.4 (Fig. 7, *A* and *B*). Interestingly, unlike the reactions with hemoglobin, these data suggest that mARC-1 may react with NO_2^- rather than HNO_2. Nevertheless, lower pH clearly increases the reaction rate; this effect could be

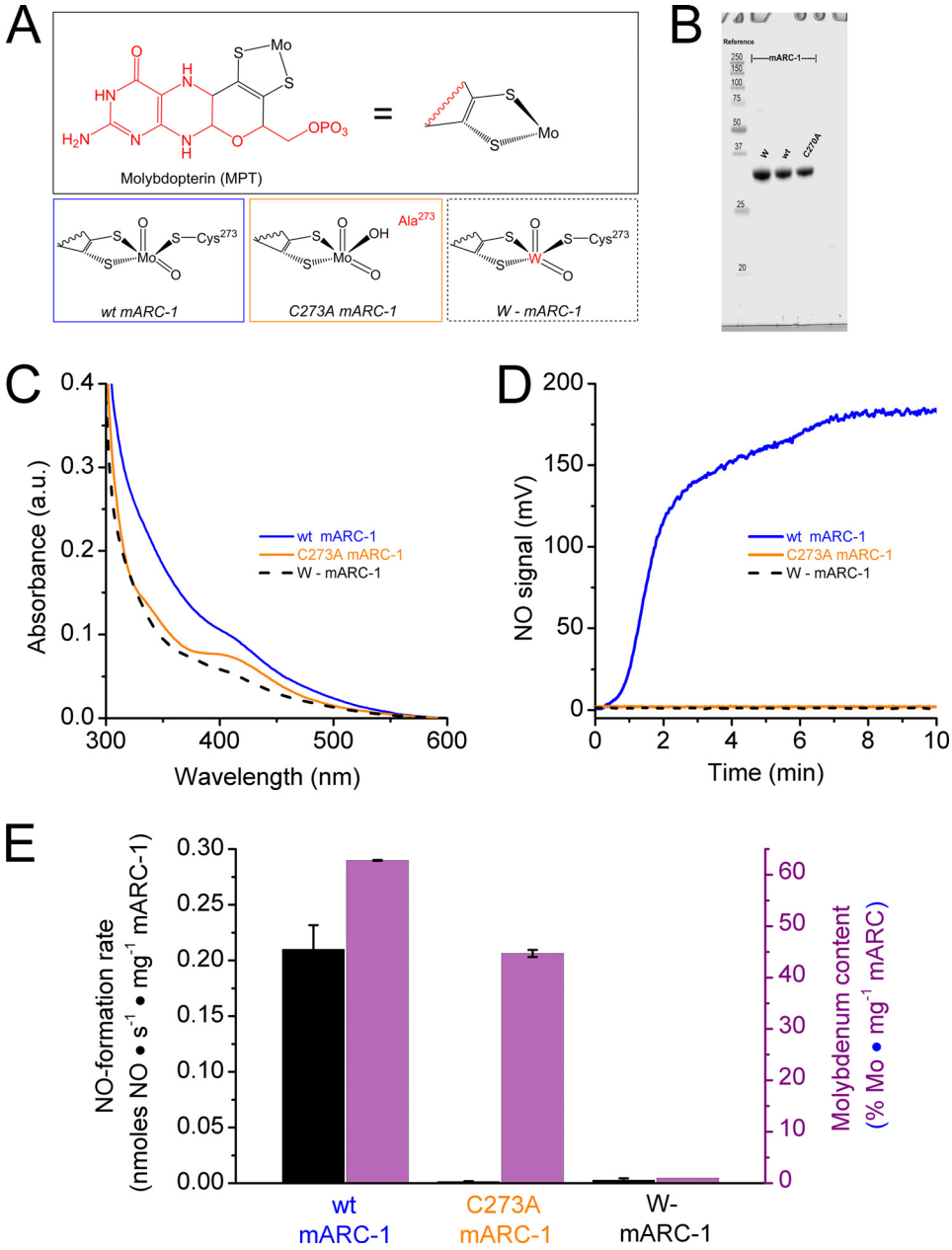

FIGURE 6. *A*, putative active site coordination of wild type (*wt*) mARC-1 and the proposed active site of mutant (*C273A*) and tungsten (*W*) mARC-1 variants used in this study. *B*, SDS/PAGE gel of enzymes isolated: W-mARC-1, wt mARC-1, C273A mARC-1. *C*, UV-visible spectra of wild type (*blue line*), C273A (*orange line*), and tungsten (*dashed black line*) mARC-1 variants generated in this study. *a.u.*, absorbance units. *D*, raw data illustrating the effect of mARC-1 active site manipulations on NO production in the NOA. *E*, summary of NO-production (*left y axis*) and molybdenum content (*right y axis*) data on mARC-1 active site variations.

related to the protonation of an active site residue and merits further investigation.

Effect of Oxygen on NO Formation Rates by mARC-1—We evaluated the effect of oxygen on nitrite reductase activity, as oxygen is known to slow nitrite reduction to NO. Oxygen inhibits NO formation from nitrite by xanthine oxidase (19) and aldehyde oxidase (21). Thus we tested the effects of amplified oxygen (21%) on mARC-1-catalyzed NO formation. We observed a clear inhibition of NO formation (Fig. 8, *A* and *B*). NO formation is inhibited by superoxide formation from oxygen by the flavin moiety of xanthine oxidoreductase (XO) and aldehyde oxidase (AO). Similarly, CYB5R, a flavin-containing enzyme, may convert oxygen into superoxide, which will react with NO forming peroxynitrite; thus peroxynitrite formation would dampen the NO signal detected. The addition of super oxide dismutase to the CYB5R, CYB5, mARC-1 enzyme reaction was able to significantly increase the NO formation activity by mARC (Fig. 8, *A* and *B*), suggesting that the superoxide formation is involved in inhibition of NO formation by mARC under aerobic conditions.

NO Formation Rates by mARC-1 and Xanthine Oxidase—Finally, we compared nitrite reduction to NO by mARC-1 with bovine xanthine oxidase, which has been shown to contribute to nitrite-NO signaling in numerous studies (36, 37). Unlike xanthine oxidase, NO formation by mARC-1 does not decrease over time (Fig. 9) but instead is stable for several minutes.

We speculate that differences in the molybdenum coordination environment between mARC and xanthine oxidase may explain the differences in NO formation profiles in the NOA. Xanthine oxidase-catalyzed nitrite reduction leads to desulfuration of the molybdenum center, irreversibly inactivating the enzyme (38); this may not be the case in human mARC, as molybdenum is coordinated by a sulfur from a cysteine side chain as in sulfite oxidase and nitrate reductase. Our experiments and others suggest that the molybdenum center is coordinated by Cys-273 sulfur in human mARC-1 (13, 27). The same was demonstrated with *C. reinhardtii* ARC. (29) We theorize that the active site difference may render mARC NO formation more stable than xanthine oxidase because it is not vulnerable to inhibition via molybdenum desulfuration.

mARC Overexpression in HEK Cells Increases NO Formation Rates—To access the applicability of mARC-catalyzed nitrite reduction to NO in eukaryotic cells, we moved our investigation to a cell culture system. HEK cells were transfected with lentivirus constructs. Overexpression of mARC was selected over silencing or deleting the gene so that the subsequent enzyme assays could be conducted well within the working range of NO detection (picomolar and higher) using a stable cell line.

A mARC:GFP fusion protein was created using a lentiviral expression vector. Fusion of mARC-2 (~35 kDa) with GFP (~25 kDa) more than doubled the molecular weight of the translated protein (Fig. 10*A*), making it easy to distinguish from endogenous mARC-1 and mARC-2 levels with a Western blot. GFP was inserted downstream from the mARC gene to preserve the N-terminal mitochondrial targeting. An analogous recombinant mARC-1:GFP was created with an N-terminal His_6 tag to simplify isolation and to confirm that the fusion of mARC and GFP would not produce a non-functional enzyme. A summary of the mARC pLVX constructs is illustrated in Fig. 10*A*.

Expression of mARC-2:GFP in lentiviral-infected HEK cells was assessed with Western blotting. HEK cells infected with empty pLVX vector (GFP only) were used as the control (Fig. 10*B*). An ~67-kDa band can be detected in the experimental group using anti-mARC2 and anti-GFP (Fig. 10*B*), indicating that the full-length mARC-2:GFP protein was expressed. An ~25-kDa band is visible in the control cells when incubated with the anti-GFP, not anti-mARC, suggesting that basal mARC-2 expression is absent in HEK cells under these growth conditions.

Next, we measured NO formation by HEK lysates. For these experiments dithionite was used as the reductant for NO formation assays with HEK cell lysates (typically 10^7 cells per assay). HEK lysate from mARC-2:GFP-expressing cells pro-

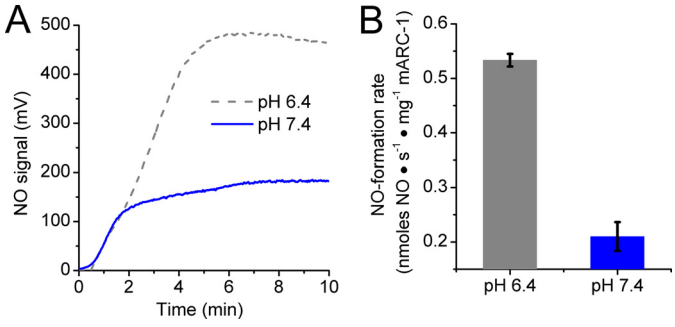

FIGURE 7. **Effect of pH and oxygen on nitrite reductase activity.** *A*, representative raw data collected from the NOA in Bis-Tris buffer, pH 6.4 and pH 7.4 Traces indicate NO production over time. *B*, NO formation rate data ($n = 3$) from experiments as shown in *panel A*. Assays carried out at 37 °C in Bis-Tris (50 mM), NADH (1 mM), nitrite (1 mM), mARC-1 (3 μM), CYB5 (2 μM), and CYB5R (0.2 μM).

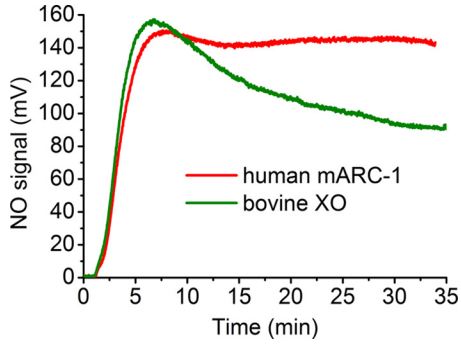

FIGURE 9. **NO formation by mARC (70 μg) and xanthine oxidase (20 μg) in 1 mM nitrite and 1 mM NADH at pH 7.4 with Bis-Tris buffer at 37 °C.** The mARC reaction also contains CYB5 (1 μM) and CYB5R (0.6 μM).

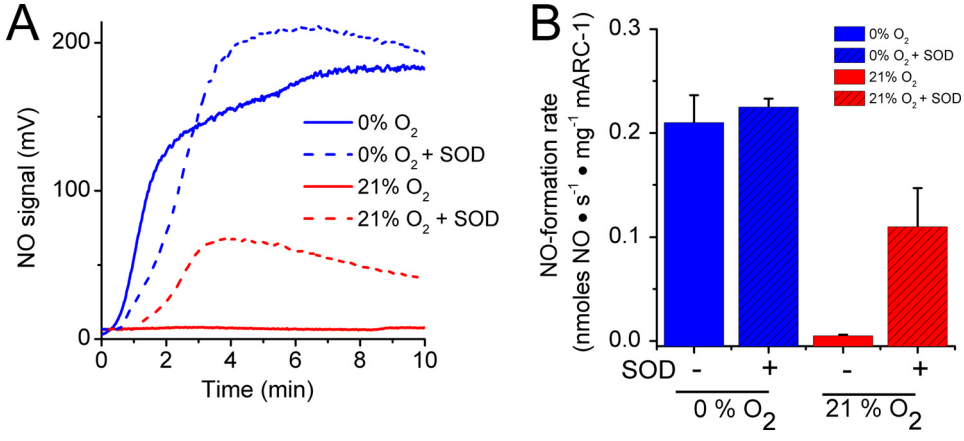

FIGURE 8. **Effect of 21% oxygen on nitrite reductase activity.** *A*, representative raw data collected from the NOA with mARC-1 in the presence (21%) or absence (0%) of oxygen. Traces indicate NO production over time. *B*, NO formation rate data ($n = 3$) from experiments performed under the anaerobic or aerobic atmosphere shown in *panel A*. Assays were carried out at 37 °C in Bis-Tris (50 mM) pH 7.4, NADH (1 mM), nitrite (1 mM), mARC-1 (3 μM), CYB5 (2 μM), and CYB5R (0.2 μM). Where indicated, super oxide dismutase (*SOD*) was added to a final concentration 60 units·ml^{-1}.

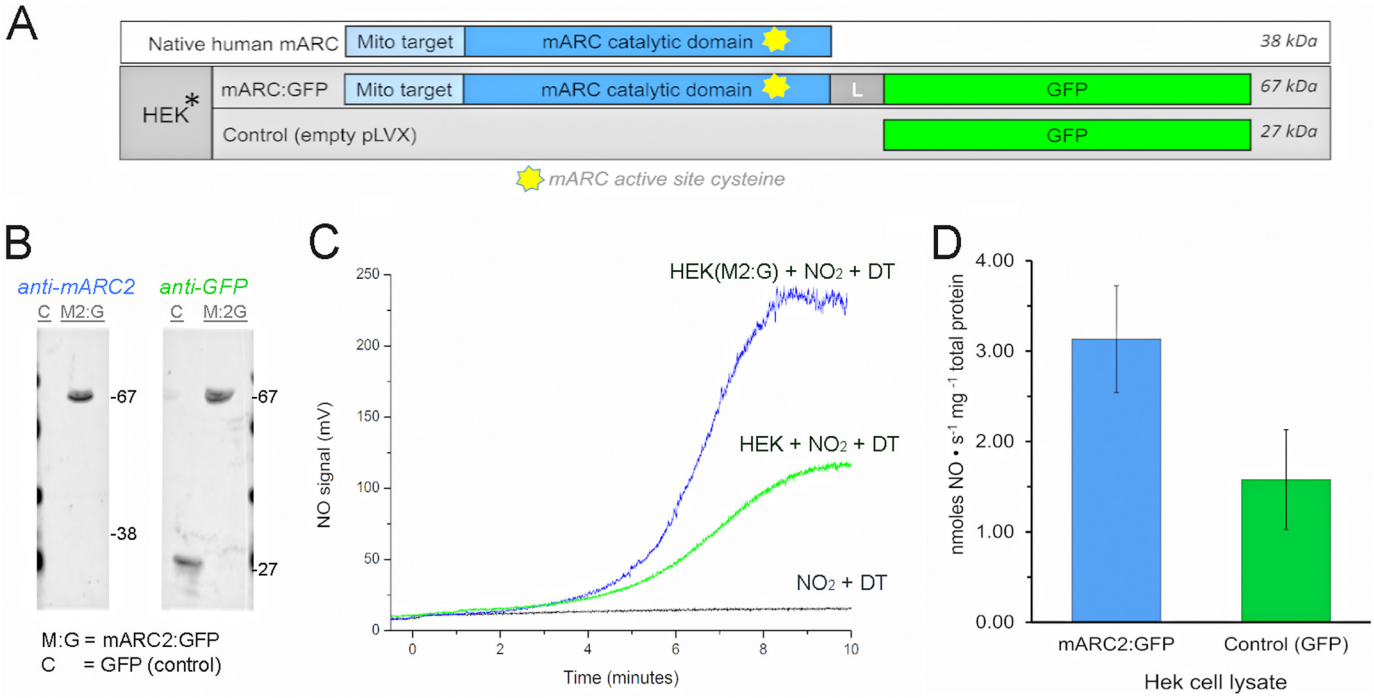

FIGURE 10. **Effect of mARC2 expression on NO production in HEK cells.** *A*, diagram summarizing mARC constructs generated for experiments with HEK (*panels B–D*). The total protein size (kDa) is listed on the *right of each construct*. Protein domains are represented by *rectangular boxes* and are not drawn to scale. The active site cysteine of mARC-1 is illustrated as a *gold star*. *B*, Western blot analysis of HEK cell lysates transformed with pLVX containing mARC-2:GFP (M:G) or GFP (empty vector control). The nitrocellulose membrane was incubated with anti-mARC-2 or anti-GFP as indicated. *C*, representative raw data collected HEK lysates expressing mARC-2:GFP or GFP (control). Traces indicate NO-production over time. Nitrite was injected to initiate the reaction at time = 0. The *black trace* represents the background rate of NO formation from the reaction of nitrite and dithionite (*DT*). *D*, NO formation rate data ($n = 3$) from experiments shown in *panel C*. Assays were carried out at 37 °C in Bis-Tris (100 mM) with dithionite (1 mM) and nitrite (10 mM) and cell lysate (50–100 mg of total).

duced significantly more NO compared with empty pLVX vector control lysates, an average of 3.2 fmol of NO·s^{-1}·mg^{-1} protein compared with 1.5 fmol of NO·s^{-1}·mg^{-1}, respectively (Fig. 10, *C* and *D*). We observed a delay in NO gas formation (Fig. 10*C*), likely reflecting NO scavenging by intracellular heme-containing proteins, enzymes, or reactive oxygen species. More work on intracellular signaling events is required to establish the physiological importance of mARC enzymes in nitrite-NO signaling.

DISCUSSION

Our knowledge about the importance of the nitrate-nitrite-NO pathway in human physiology and therapeutics has advanced considerably in recent years, with an established role in blood pressure regulation, hypoxic vasodilation, and energetics (2). However, the precise subcellular regulation of nitrite reduction and the enzymes that participate in this process remain incompletely characterized.

At this time most of the literature available on nitrite reduction to NO by mammalian molybdopterin enzymes has focused on xanthine oxidase (37, 39–45). Inhibition of xanthine oxidase by purine analogues (*e.g.* allopurinol, oxypurinol) or other inhibitors such as febuxostat has facilitated research into the role of xanthine oxidase as a NO-forming nitrite reductase. Clearly, xanthine oxidase contributes to nitrite reduction and the signaling and therapeutic effects of nitrite in murine lung and vascular system (36, 37, 46). However, xanthine oxidase is not the major nitrite reductase in humans, as xanthine oxidase inhibition using co-infusions of oxypurinol does not inhibit

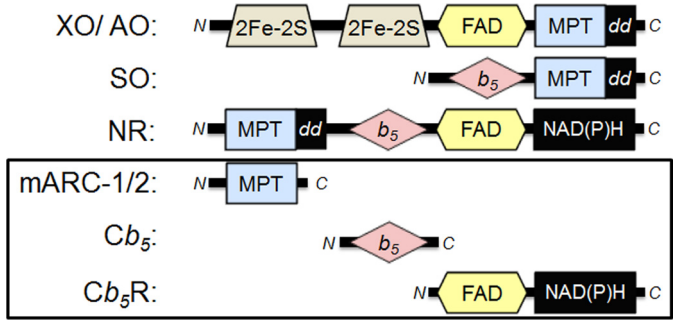

FIGURE 11. **Redox-active centers of eukaryotic molybdenum enzymes.** Human XO, human AO, human sulfite oxidase (*SO*), plant nitrate reductase (*NR*), and human mARC. Linear protein sequences are represented as a *solid black line* with flanking N and C termini labels. The human CYB5 and CYB5R are included to illustrate the similarities and differences among eukaryotic molybdenum-dependent enzymes and the mARC complex. Redox-active sites are depicted as colored geometric shapes: iron-sulfur cluster (*2Fe-2S*), FAD, molybdopterin (*MPT*), and b-type heme (b_5). Nitrate reductase (*NR*) and CYB5R also contain a NAD(P)H binding domain (*black square*). The molybdopterin dimerization domain (*dd*) is depicted as a *black box*.

nitrite-dependent vasodilation in healthy humans (47). Current evidence suggests that the vascular nitrite reductase activity is controlled by deoxyhemoglobin and/or deoxymyoglobin; however, it is possible that other vascular nitrite reductases have not yet been discovered. These observations prompted us to investigate mARC as a candidate NO-forming nitrite reductase.

The human mARC enzymes have only recently been identified as the fourth human molybdopterin enzyme and were annotated as mosc1 and mosc2 for several years based on primary sequence homology with the molybdenum cofactor sul-

furase C-terminal domain. Together, mARC, CYB5, and CYB5R enzymes contain analogous redox-active sites to the plant nitrate reductase (27) (Fig. 11), which contains molybdopterin, b_5-typeheme, flavin adenine dinucleotide (FAD), and nicotinamide adenine dinucleotide (NADH) binding domains. We, therefore, hypothesized that the mitochondrial amidoxime-reducing complex, which is composed of a mARC, CYB5, and CYB5R metabolon, may play an important role in mitochondrial nitrite reduction to NO.

In this study we examine the function of human mARC-1 and mARC-2 as NO-forming nitrite reductases. Our data clearly indicated that mARC enzymes are able to catalyze nitrite reduction, with CYB5 and CYB5R forming the reconstituted reductase complex. Based on our data, mARC may contribute to the observed nitrite reductase activity of intact mitochondria. It should be noted that in hypoxic conditions the concentrations of NADH increase, which may lead to reduction of mARC and enhanced nitrite reduction to NO. This provides a potential new physiological pathway for nitrite reduction to NO under hypoxia.

Molybdopterin enzymes have an intrinsic ability to reduce nitrite into NO (Table 1). Although no molybdopterin enzyme has been annotated as a dedicated "nitrite reductase," several studies have shown independently that the mammalian molybdopterin enzymes aldehyde oxidase (21) and xanthine oxidase (34) catalyze nitrite reduction to NO. These observations prompted us to investigate mARC as a candidate NO-forming nitrite reductase. Herein we show that mARC-1 can metabolize nitrite into NO. Comparison of mARC-1 kinetic constants with published values reveals that mARC-1 has a moderate nitrite affinity, similar to XO, which has been shown to signal both *in vitro* and *in vivo*.

After establishing that mARC-1 was able to reduce nitrite into NO, we wanted to determine the mechanism for mARC-1-dependent nitrite reduction. In xanthine oxidase and aldehyde oxidase, the molybdopterin active site is the location of nitrite reduction to NO. Presumably, the oxygen atom of the nitrite anion is transferred to molybdenum via an oxygen atom transfer reaction, releasing NO (49). The molybdopterin active site of mARC is similar to xanthine oxidase with one central difference, xanthine oxidase and aldehyde oxidase contain a sulfido ligand, whereas mARC and sulfite oxidase use as the ligand the sulfur atom of a cysteine side-chain, Cys-273 mARC-1 and Cys272 mARC-2, which is strictly conserved in eukaryotic and prokaryotic mARC homologues (29). We show that the mutation of mARC-1 Cys-273 to alanine abolished NO formation, in agreement with the previous reports evaluating the amidoxime reductase activity of human (27) and *C. reinhardtii* (29) ARC enzymes. In our hands C273A mutation did not significantly disrupt molybdenum binding, consistent with the structurally characterized sulfite oxidase Cys-Ala mutant. We expect that mARC C273A mutant active site would create an inactive tri-oxo coordinated molybdenum, as demonstrated with sulfite oxidase cysteine to alanine and serine mutants (28, 50).

We also created tungsten-substituted mARC-1 to demonstrate that the molybdenum active site is required for NO formation. Tungsten, a group VI transition metal like molybdenum, can be selectively incorporated into the dithiolene groups of the molybdopterin cofactor in *E. coli* (51, 52); however, eukaryotic molybdenum enzymes, such as nitrate reductase (18) and sulfite oxidase (26), are strongly inhibited by tungsten. Tungsten reverses the protective effects of nitrite in hypoxia induced pulmonary arterial hypertension (37). W-mARC-1 was inactive, again suggesting that the molybdenum active site of mARC-1 is the site of nitrite reduction to NO. Tungsten is elevated in the urine of individuals with peripheral arterial disease (53); thus, it is possible that mARC enzymes mediate the therapeutic effects of nitrite and NO in peripheral arterial disease (54).

Additionally, we demonstrate that mARC-1 and mARC-2 are the NO-producing components by measuring nitrite reduction to NO in the absence of CYB5 and CYB5R enzymes. mARC does not react with NADH at detectable rates; therefore, a nonspecific reductant, dithionite, was used. As demonstrated with the NADH-linked reductase system, NO formation accelerates with increasing nitrite concentrations. The reaction is dependent on active enzyme, as the denatured mARC is unreactive. Furthermore, CYB5, CYB5R, and NADH, without mARC, do not reduce nitrite to NO. This suggests that mARC is the catalytic subunit with flexibility to accept electrons from a pool of electron donors.

Nitrite reduction to NO is increased at low pH (high H^+) and low oxygen (hypoxia). Thus, we tested the effects on NO formation with mARC-1, CYB5, CYB5R, and NADH. Decreasing pH values increase the activity of mARC catalyzed NO formation from nitrite. Data show a dramatic drop in NO formation in the presence of oxygen. It is possibly a result of molybdenum oxidation, as the fully oxidized molybdenum (Mo(VI)) would not be able to reduce nitrite. As the reaction mixture contains excess NADH, this would indicate that the reducing system is not efficient enough to keep the molybdenum reduced. Moreover, oxygen inhibition appears to be associated with the formation of superoxide (O_2^-), as the addition of super oxide dismutase to the reaction mixture can elevate the inhibitory effect of oxygen on NO formation by mARC-1. CYB5R is the most likely source of O_2^-, as reduced flavins, such as the FAD cofactor of CYB5R, can produce O_2^- in the presence of oxygen. Superoxide production by the FAD moiety of XO is a significant source of reactive oxygen species *in vivo*, especially during ischemic injury.

mARC enzymes are widely expressed in human tissue, and mARC-1 and mARC-2 have different distributions in tissue (27), possibly suggesting that both enzymes fulfill different physiological functions. Despite the ability of mARC to catalyze reduction of amidoxime groups *in vitro*, the physiological function of mARC is not clear. Both were annotated as mosc1 and mosc2 for several years based on primary sequence homology with the molybdenum cofactor sulfurase C-terminal domain. Later, mARC-1 and mARC-2 enzymes have been shown to catalyze reduction of *N*-hydroxylated nitrogen groups on a variety of compounds (55) with both recombinant enzymes and cells (56); however, the significance of mARC enzymes in the *in vivo* transformation of hydroxylamines have not been established. mARC has also been proposed to modulate NO availability, as it can reduce N^{ω}-hydroxy-L-arginine into L-arginine (25). N^{ω}-Hydroxy-L-arginine is a potent arginase inhibitor and intermedi-

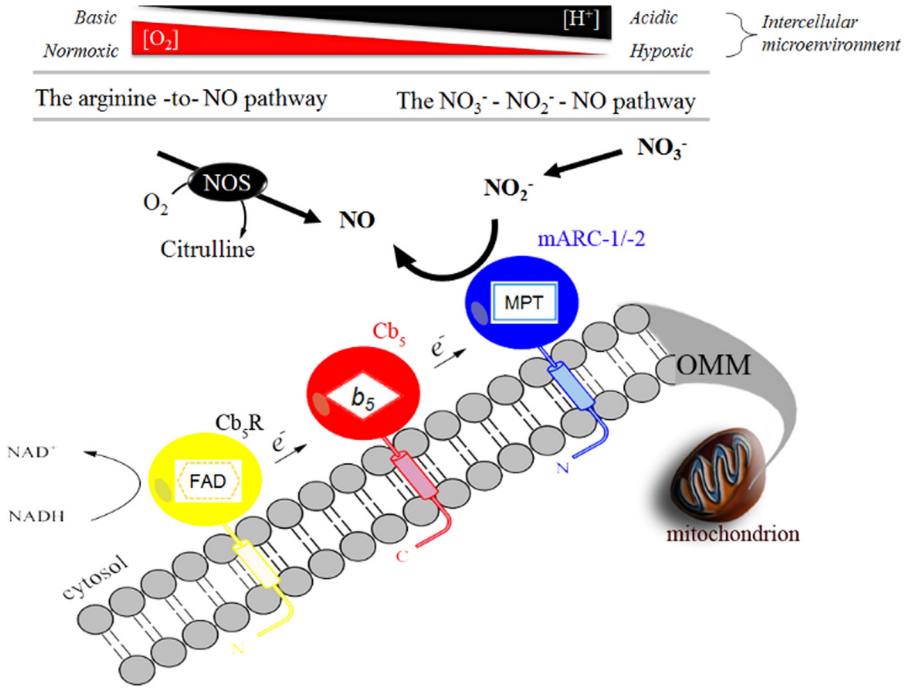

FIGURE 12. **Two pathways of NO biosynthesis in humans.** The formation of NO from arginine and the reduction of nitrite to NO through the mARC/CB5/CB5R pathway are shown. The proteins involved are depicted as *ovals*. *OMM*, outer mitochondrial membrane; *FAD*, flavin adenine dinucleotide; *MPT*, molybdopterin.

ate in the conversion of arginine to citrulline and NO by nitric-oxide synthase. Further studies will be required to establish the primary and secondary functions of these enzymes *in vivo*, as either deaminases or nitrite reductases.

mARC enzymes are embedded in the outer mitochondrial membrane facing the cytosol (13, 14). Both mARC-1 and mARC-2 encoded a large (~50 amino acid) N-terminal mitochondrial signal sequence, which is used to anchor mARC onto the mitochondrial surface (Fig. 12). The cytosolic face may be an advantageous location for this perspective mitochondrial nitrite reductase, as nitrite diffusion is limited across the outer mitochondrial membrane (14). These data demonstrate that mARC transforms nitrite to NO at higher rates than cytochrome *c* and other previously studied reductases (57) (see also Table 1). The second-order rate constants for the nitrite reductase activity of ferrous horse heart cytochrome *c* was reported recently to be 7.0×10^{-2} M^{-1} s^{-1} (57). Mitochondria are known to metabolize nitrite into NO (5, 8, 58). A number of studies have suggested different sites of reduction (11, 59, 60); cytochrome *c* (11), complex III (5), and complex IV (10) have been reported to reduce nitrite into NO as well as mitochondria-associated deoxymyoglobin and ubiquinol (9). However, these pathways may be limited at physiological pH values (10) and by slow nitrite anion diffusion through the outer mitochondrial membrane to the inner mitochondrial membrane.

The role of mARC-1 in cardiovascular disease is not clear. In humans, mARC-1 RNA expression decreases in response to controlled reoxygenation after cardiopulmonary bypass surgery (62). Analysis of the NextBio database (63) for expression changes in mARC-1 and mARC-2 revealed that mARC-2 expression is down-regulated in response to hypoxia in mice (data were collected from Gharib *et al.* (61)). Taken together, this suggests that mARC expression maybe regulated in response to changes in oxygen tension; however, more studies need to be conducted to investigate the significance of this.

In conclusion, our studies suggest that mARC-1 and mARC-2 catalyze NADH-dependent nitrite reduction to NO at the molybdenum active site under anaerobic conditions in the presence of CYB5 and CYB5R. Nitric oxide formation was abolished in 21% oxygen but was enhanced at low pH. Additional studies are indicated to explore a possible role for mARC in physiological and therapeutic nitrite-NO signaling.

Acknowledgments—We thank Mario Rivera (University of Kansas) for providing the CYB5 expression plasmid and Tracy Palmer (University of Dundee) for providing the pTPR1 MOCO biosynthesis plasmid.

REFERENCES

1. Gladwin, M. T., Raat, N. J., Shiva, S., Dezfulian, C., Hogg, N., Kim-Shapiro, D. B., and Patel, R. P. (2006) Nitrite as a vascular endocrine nitric oxide reservoir that contributes to hypoxic signaling, cytoprotection, and vasodilation. *Am. J. Physiol. Heart Circ. Physiol.* **291,** H2026–H2035
2. Lundberg, J. O., Weitzberg, E., and Gladwin, M. T. (2008) The nitrate-nitrite-nitric oxide pathway in physiology and therapeutics. *Nat. Rev. Drug Discov.* **7,** 156–167
3. Sparacino-Watkins, C., Stolz, J. F., and Basu, P. (2014) Nitrate and periplasmic nitrate reductases. *Chem. Soc. Rev.* **43,** 676–706
4. Kozlov, A. V., Staniek, K., and Nohl, H. (1999) Nitrite reductase activity is a novel function of mammalian mitochondria. *FEBS Lett.* **454,** 127–130
5. Nohl, H., Staniek, K., Sobhian, B., Bahrami, S., Redl, H., and Kozlov, A. V. (2000) Mitochondria recycle nitrite back to the bioregulator nitric monoxide. *Acta Biochim. Pol.* **47,** 913–921
6. Bueno, M., Wang, J., Mora, A. L., and Gladwin, M. T. (2013) Nitrite signaling in pulmonary hypertension. Mechanisms of bioactivation, signaling, and therapeutics. *Antioxid. Redox Signal.* **18,** 1797–1809
7. Sparacino-Watkins, C. E., Lai, Y.-C., and Gladwin, M. T. (2012) Nitrate-nitrite-nitric oxide pathway in pulmonary arterial hypertension therapeu-

tics. *Circulation* **125,** 2824–2826
8. Shiva, S. (2010) Mitochondria as metabolizers and targets of nitrite. *Nitric Oxide* **22,** 64–74
9. Shiva, S., Huang, Z., Grubina, R., Sun, J., Ringwood, L. A., MacArthur, P. H., Xu, X., Murphy, E., Darley-Usmar, V. M., and Gladwin, M. T. (2007) Deoxymyoglobin is a nitrite reductase that generates nitric oxide and regulates mitochondrial respiration. *Circ. Res.* **100,** 654–661
10. Castello, P. R., David, P. S., McClure, T., Crook, Z., and Poyton, R. O. (2006) Mitochondrial cytochrome oxidase produces nitric oxide under hypoxic conditions. Implications for oxygen sensing and hypoxic signaling in eukaryotes. *Cell Metab.* **3,** 277–287
11. Basu, S., Azarova, N. A., Font, M. D., King, S. B., Hogg, N., Gladwin, M. T., Shiva, S., and Kim-Shapiro, D. B. (2008) Nitrite Reductase activity of cytochrome *c*. *J. Biol. Chem.* **283,** 32590–32597
12. Havemeyer, A., Bittner, F., Wollers, S., Mendel, R., Kunze, T., and Clement, B. (2006) Identification of the missing component in the mitochondrial benzamidoxime prodrug-converting system as a novel molybdenum enzyme. *J. Biol. Chem.* **281,** 34796–34802
13. Wahl, B., Reichmann, D., Niks, D., Krompholz, N., Havemeyer, A., Clement, B., Messerschmidt, T., Rothkegel, M., Biester, H., Hille, R., Mendel, R. R., and Bittner, F. (2010) Biochemical and spectroscopic characterization of the human mitochondrial amidoxime reducing components hmARC-1 and hmARC-2 suggests the existence of a new molybdenum enzyme family in eukaryotes. *J. Biol. Chem.* **285,** 37847–37859
14. Klein, J. M., Busch, J. D., Potting, C., Baker, M. J., Langer, T., and Schwarz, G. (2012) The mitochondrial amidoxime-reducing component (mARC1) is a novel signal-anchored protein of the outer mitochondrial membrane. *J. Biol. Chem.* **287,** 42795–42803
15. Ozols, J. (1974) Cytochrome b5 from microsomal membranes of equine, bovine, and porcine livers. Isolation and properties of preparations containing the membranous segment. *Biochemistry* **13,** 426–434
16. Shirabe, K., Yubisui, T., and Takeshita, M. (1989) Expression of human erythrocyte NADH-cytochrome b5 reductase as an α-thrombin-cleavable fused protein in *Escherichia coli*. *Biochim. Biophys. Acta* **1008,** 189–192
17. Altuve, A., Wang, L., Benson, D. R., and Rivera, M. (2004) Mammalian mitochondrial and microsomal cytochromes b5 exhibit divergent structural and biophysical characteristics. *Biochem. Biophys. Res. Commun.* **314,** 602–609
18. Pollock, V. V., Conover, R. C., Johnson, M. K., and Barber, M. J. (2002) Bacterial expression of the molybdenum domain of assimilatory nitrate reductase. Production of both the functional molybdenum-containing domain and the nonfunctional tungsten analog. *Arch. Biochem. Biophys.* **403,** 237–248
19. Li, H., Samouilov, A., Liu, X., and Zweier, J. L. (2004) Characterization of the effects of oxygen on xanthine oxidase-mediated nitric oxide formation. *J. Biol. Chem.* **279,** 16939–16946
20. Li, H., Samouilov, A., Liu, X., and Zweier, J. L. (2001) Characterization of the magnitude and kinetics of xanthine oxidase-catalyzed nitrite reduction. Evaluation of its role in nitric oxide generation in anoxic tissues. *J. Biol. Chem.* **276,** 24482–24489
21. Li, H., Kundu, T. K., and Zweier, J. L. (2009) Characterization of the magnitude and mechanism of aldehyde oxidase-mediated nitric oxide production from nitrite. *J. Biol. Chem.* **284,** 33850–33858
22. Pai, T. G., Payne, W. J., and LeGall, J. (1987) Use of a chemiluminescence detector for quantitation of nitric oxide produced in assays of denitrifying enzymes. *Anal. Biochem.* **166,** 150–157
23. MacArthur, P. H., Shiva, S., and Gladwin, M. T. (2007) Measurement of circulating nitrite and *S*-nitrosothiols by reductive chemiluminescence. *J. Chromatogr. B Analyt. Technol. Biomed. Life Sci.* **851,** 93–105
24. Millar, T. M., Stevens, C. R., Benjamin, N., Eisenthal, R., Harrison, R., and Blake, D. R. (1998) Xanthine oxidoreductase catalyses the reduction of nitrates and nitrite to nitric oxide under hypoxic conditions. *FEBS Lett.* **427,** 225–228
25. Kotthaus, J., Wahl, B., Havemeyer, A., Kotthaus, J., Schade, D., Garbe-Schönberg, D., Mendel, R., Bittner, F., and Clement, B. (2011) Reduction of Nω-hydroxy-L-arginine by the mitochondrial amidoxime reducing component (mARC). *Biochem. J.* **433,** 383–391
26. Johnson, J. L., Hainline, B. E., Rajagopalan, K. V., and Arison, B. H. (1984) The pterin component of the molybdenum cofactor. Structural characterization of two fluorescent derivatives. *J. Biol. Chem.* **259,** 5414–5422
27. Havemeyer, A., Lang, J., and Clement, B. (2011) The fourth mammalian molybdenum enzyme mARC. Current state of research. *Drug Metab. Rev.* **43,** 524–539
28. Qiu, J. A., Wilson, H. L., Pushie, M. J., Kisker, C., George, G. N., and Rajagopalan, K. V. (2010) The structures of the C185S and C185A mutants of sulfite oxidase reveal rearrangement of the active site. *Biochemistry* **49,** 3989–4000
29. Chamizo-Ampudia, A., Galvan, A., Fernandez, E., and Llamas, A. (2011) The *Chlamydomonas reinhardtii* molybdenum cofactor enzyme crARC has a Zn-dependent activity and protein partners similar to those of its human homologue. *Eukaryot. Cell* **10,** 1270–1282
30. Tiso, M., Tejero, J., Basu, S., Azarov, I., Wang, X., Simplaceanu, V., Frizzell, S., Jayaraman, T., Geary, L., Shapiro, C., Ho, C., Shiva, S., Kim-Shapiro, D. B., and Gladwin, M. T. (2011) Human neuroglobin functions as a redox-regulated nitrite reductase. *J. Biol. Chem.* **286,** 18277–18289
31. Doyle, M. P., Pickering, R. A., DeWeert, T. M., Hoekstra, J. W., and Pater, D. (1981) Kinetics and mechanism of the oxidation of human deoxyhemoglobin by nitrites. *J. Biol. Chem.* **256,** 12393–12398
32. Huang, Z., Shiva, S., Kim-Shapiro, D. B., Patel, R. P., Ringwood, L. A., Irby, C. E., Huang, K. T., Ho, C., Hogg, N., Schechter, A. N., and Gladwin, M. T. (2005) Enzymatic function of hemoglobin as a nitrite reductase that produces NO under allosteric control. *J. Clin. Invest.* **115,** 2099–2107
33. Doyle, M. P., Pickering, R. A., and da Conceição, J. (1984) Structural effects in alkyl nitrite oxidation of human hemoglobin. *J. Biol. Chem.* **259,** 80–87
34. Li, H., Samouilov, A., Liu, X., and Zweier, J. L. (2003) Characterization of the magnitude and kinetics of xanthine oxidase-catalyzed nitrate reduction. Evaluation of its role in nitrite and nitric oxide generation in anoxic tissues. *Biochemistry* **42,** 1150–1159
35. Wang, J., Krizowski, S., Fischer, K., Niks, D., Tejero, J., Wang, L., Sparacino-Watkins, C., Ragireddy, P., Frizzell, S., Kelley, E. E., Shiva, S., Zhang, Y., Basu, P., Hille, R., Schwarz, G., and Gladwin, M. T. (2013) P62. Sulfite oxidase catalyzes single electron transfer at molybdenum domain to reduce nitrite to NO. *Nitric Oxide* **31,** S39–S40
36. Baliga, R. S., Milsom, A. B., Ghosh, S. M., Trinder, S. L., Macallister, R. J., Ahluwalia, A., and Hobbs, A. J. (2012) Dietary nitrate ameliorates pulmonary hypertension: cytoprotective role for endothelial nitric-oxide synthase and xanthine oxidoreductase. *Circulation* **125,** 2922–2932
37. Zuckerbraun, B. S., Shiva, S., Ifedigbo, E., Mathier, M. A., Mollen, K. P., Rao, J., Bauer, P. M., Choi, J. J., Curtis, E., Choi, A. M., and Gladwin, M. T. (2010) Nitrite potently inhibits hypoxic and inflammatory pulmonary arterial hypertension and smooth muscle proliferation via xanthine oxidoreductase-dependent nitric oxide generation. *Circulation* **121,** 98–109
38. Harrison, R. (2002) Structure and function of xanthine oxidoreductase. Where are we now? *Free Radic. Biol. Med.* **33,** 774–797
39. Samal, A. A., Honavar, J., Brandon, A., Bradley, K. M., Doran, S., Liu, Y., Dunaway, C., Steele, C., Postlethwait, E. M., Squadrito, G. L., Fanucchi, M. V., Matalon, S., and Patel, R. P. (2012) Administration of nitrite after chlorine gas exposure prevents lung injury. Effect of administration modality. *Free Radic. Biol. Med.* **53,** 1431–1439
40. Pickerodt, P. A., Emery, M. J., Zarndt, R., Martin, W., Francis, R. C., Boemke, W., and Swenson, E. R. (2012) Sodium nitrite mitigates ventilator-induced lung injury in rats. *Anesthesiology* **117,** 592–601
41. Sugimoto, R., Okamoto, T., Nakao, A., Zhan, J., Wang, Y., Kohmoto, J., Tokita, D., Farver, C. F., Tarpey, M. M., Billiar, T. R., Gladwin, M. T., and McCurry, K. R. (2012) Nitrite reduces acute lung injury and improves survival in a rat lung transplantation model. *Am. J. Transplant.* **12,** 2938–2948
42. Baker, J. E., Su, J., Fu, X., Hsu, A., Gross, G. J., Tweddell, J. S., and Hogg, N. (2007) Nitrite confers protection against myocardial infarction. Role of xanthine oxidoreductase, NADPH oxidase. and K(ATP) channels. *J. Mol. Cell. Cardiol.* **43,** 437–444
43. Webb, A., Bond, R., McLean, P., Uppal, R., Benjamin, N., and Ahluwalia, A. (2004) Reduction of nitrite to nitric oxide during ischemia protects against myocardial ischemia-reperfusion damage. *Proc. Natl. Acad. Sci. U.S.A.* **101,** 13683–13688
44. Lu, P., Liu, F., Yao, Z., Wang, C. Y., Chen, D. D., Tian, Y., Zhang, J. H., and

Wu, Y. H. (2005) Nitrite-derived nitric oxide by xanthine oxidoreductase protects the liver against ischemia-reperfusion injury. *Hepatobiliary Pancreat. Dis. Int.* **4,** 350–355
45. Alef, M. J., Vallabhaneni, R., Carchman, E., Morris, S. M., Jr., Shiva, S., Wang, Y., Kelley, E. E., Tarpey, M. M., Gladwin, M. T., Tzeng, E., and Zuckerbraun, B. S. (2011) Nitrite-generated NO circumvents dysregulated arginine/NOS signaling to protect against intimal hyperplasia in Sprague-Dawley rats. *J. Clin. Invest.* **121,** 1646–1656
46. Webb, A. J., Patel, N., Loukogeorgakis, S., Okorie, M., Aboud, Z., Misra, S., Rashid, R., Miall, P., Deanfield, J., Benjamin, N., MacAllister, R., Hobbs, A. J., and Ahluwalia, A. (2008) Acute blood pressure lowering, vasoprotective, and antiplatelet properties of dietary nitrate via bioconversion to nitrite. *Hypertension* **51,** 784–790
47. Dejam, A., Hunter, C. J., Tremonti, C., Pluta, R. M., Hon, Y. Y., Grimes, G., Partovi, K., Pelletier, M. M., Oldfield, E. H., Cannon, R. O., 3rd., Schechter, A. N., and Gladwin, M. T. (2007) Nitrite infusion in humans and nonhuman primates. *Circulation* **116,** 1821–1831
48. Tan, S., Yokoyama, Y., Dickens, E., Cash, T. G., Freeman, B. A., and Parks, D. A. (1993) Xanthine oxidase activity in the circulation of rats following hemorrhagic shock. *Free Radic. Biol. Med.* **15,** 407–414
49. Maia, L. B., and Moura, J. J. (2011) Nitrite reduction by xanthine oxidase family enzymes. A new class of nitrite reductases. *J. Biol. Inorg. Chem* **16,** 443–460
50. Garrett, R. M., and Rajagopalan, K. V. (1996) Site-directed mutagenesis of recombinant sulfite oxidase. Identification of cysteine 207 as a ligand of molybdenum. *J. Biol. Chem.* **271,** 7387–7391
51. Neumann, M., and Leimkühler, S. (2008) Heavy metal ions inhibit molybdoenzyme activity by binding to the dithiolene moiety of molybdopterin in *Escherichia coli*. *FEBS J.* **275,** 5678–5689
52. Mendel, R. R., and Schwarz, G. (2011) Molybdenum cofactor biosynthesis in plants and humans. *Coord. Chem. Rev.* **255,** 1145–1158
53. Navas-Acien, A., Silbergeld, E. K., Sharrett, R., Calderon-Aranda, E., Selvin, E., and Guallar, E. (2005) Metals in urine and peripheral arterial disease. *Environ. Health Perspect.* **113,** 164–169
54. Allen, J. D., Giordano, T., and Kevil, C. G. (2012) Nitrite and nitric oxide metabolism in peripheral artery disease. *Nitric Oxide* **26,** 217–222
55. Gruenewald, S., Wahl, B., Bittner, F., Hungeling, H., Kanzow, S., Kotthaus, J., Schwering, U., Mendel, R. R., and Clement, B. (2008) The fourth molybdenum containing enzyme mARC. Cloning and involvement in the activation of *N*-hydroxylated prodrugs. *J. Med. Chem.* **51,** 8173–8177
56. Plitzko, B., Ott, G., Reichmann, D., Henderson, C. J., Wolf, C. R., Mendel, R., Bittner, F., Clement, B., and Havemeyer, A. (2013) The involvement of mitochondrial amidoxime reducing components 1 and 2 and mitochondrial cytochrome b5 in *N*-reductive metabolism in human cells. *J. Biol. Chem.* **288,** 20228–20237
57. Ascenzi, P., Tundo, G. R., Fanali, G., Coletta, M., and Fasano, M. (2013) Warfarin modulates the nitrite reductase activity of ferrous human serum heme-albumin. *J. Biol. Inorg. Chem.* **18,** 939–946
58. Shiva, S., Sack, M. N., Greer, J. J., Duranski, M., Ringwood, L. A., Burwell, L., Wang, X., MacArthur, P. H., Shoja, A., Raghavachari, N., Calvert, J. W., Brookes, P. S., Lefer, D. J., and Gladwin, M. T. (2007) Nitrite augments tolerance to ischemia/reperfusion injury via the modulation of mitochondrial electron transfer. *J. Exp. Med.* **204,** 2089–2102
59. Nohl, H., Staniek, K., and Kozlov, A. V. (2005) The existence and significance of a mitochondrial nitrite reductase. *Redox Rep.* **10,** 281–286
60. Poyton, R. O., and Ball, K. A. (2011) Therapeutic photobiomodulation. Nitric oxide and a novel function of mitochondrial cytochrome *c* oxidase. *Discov Med.* **11,** 154–159
61. Gharib, S. A., Luchtel, D. L., Madtes, D. K., and Glenny, R. W. (2005) Global gene annotation analysis and transcriptional profiling identify key biological modules in hypoxic pulmonary hypertension. *Physiol Genomics* **22,** 14–23
62. Ghorbel, M. T., Mokhtari, A., Sheikh, M., Angelini, G. D., and Caputo, M. (2012) Controlled reoxygenation cardiopulmonary bypass is associated with reduced transcriptomic changes in cyanotic tetralogy of Fallot patients undergoing surgery. *Physiol. Genomics* **44,** 1098–1106
63. Kupershmidt, I., Su, Q. J., Grewal, A., Sundaresh, S., Halperin, I., Flynn, J., Shekar, M., Wang, H., Park, J., Cui, W., Wall, G. D., Wisotzkey, R., Alag, S., Akhtari, S., and Ronaghi, M. (2010) Ontology-based meta-analysis of global collections of high-throughput public data. *PloS ONE* **5,** e13066